

# **Supporting Information for**

## **Design of the new closo-dodecarborate-containing gemcitabine analogue for the albumin-based theranostics composition.**

**Valeria I. Raskolupova<sup>1</sup>, Meiling Wang<sup>2</sup>, Maya A. Dymova<sup>1</sup>, Gleb O. Petrov<sup>1</sup>, Ivan M. Shchudlo<sup>3</sup>, Sergey Yu. Taskaev<sup>2,3</sup>, Tatyana V. Abramova<sup>1</sup>, Tatyana S. Godovikova<sup>1,2</sup>, Vladimir N. Silnikov<sup>1</sup>, Tatyana V. Popova<sup>1,2\*</sup>.**

- <sup>1</sup> Institute of Chemical Biology and Fundamental Medicine, SB RAS, 630090 Novosibirsk, Russia;  
v.raskolupova@mail.ru (V.I.R.); maya.a.rot@gmail.com (M.A.D.); [petrov.olegovich@gmail.com](mailto:petrov.olegovich@gmail.com) (G.O.P.)  
t\_godovikova@mail.ru (T.S.G); abramova@niboch.nsc.ru (T.V.A.); silnik@niboch.nsc.ru (V.N.S.);  
io197724@gmail.com (T.V.P.)
- <sup>2</sup> Novosibirsk State University, Faculty of Natural Sciences, 630090 Novosibirsk, Russia;  
io197724@gmail.com (T.V.P.); 153890812@qq.com (M.V.); s.yu.taskaev@inp.nsk.su (S.Yu.T.)
- <sup>3</sup> Budker Institute of Nuclear Physics, SB RAS, 630090 Novosibirsk, Russia; s.yu.taskaev@inp.nsk.su  
(S.Yu.T.); [cshudlo.i.m@gmail.com](mailto:cshudlo.i.m@gmail.com) (I.M.S.)
- \* Correspondence: io197724@gmail.ru; Tel.: +8-383-3635183

## Spectral data for new compounds

4-N-benzoyl-2'-deoxy-2',2'-difluorocytidine (2)

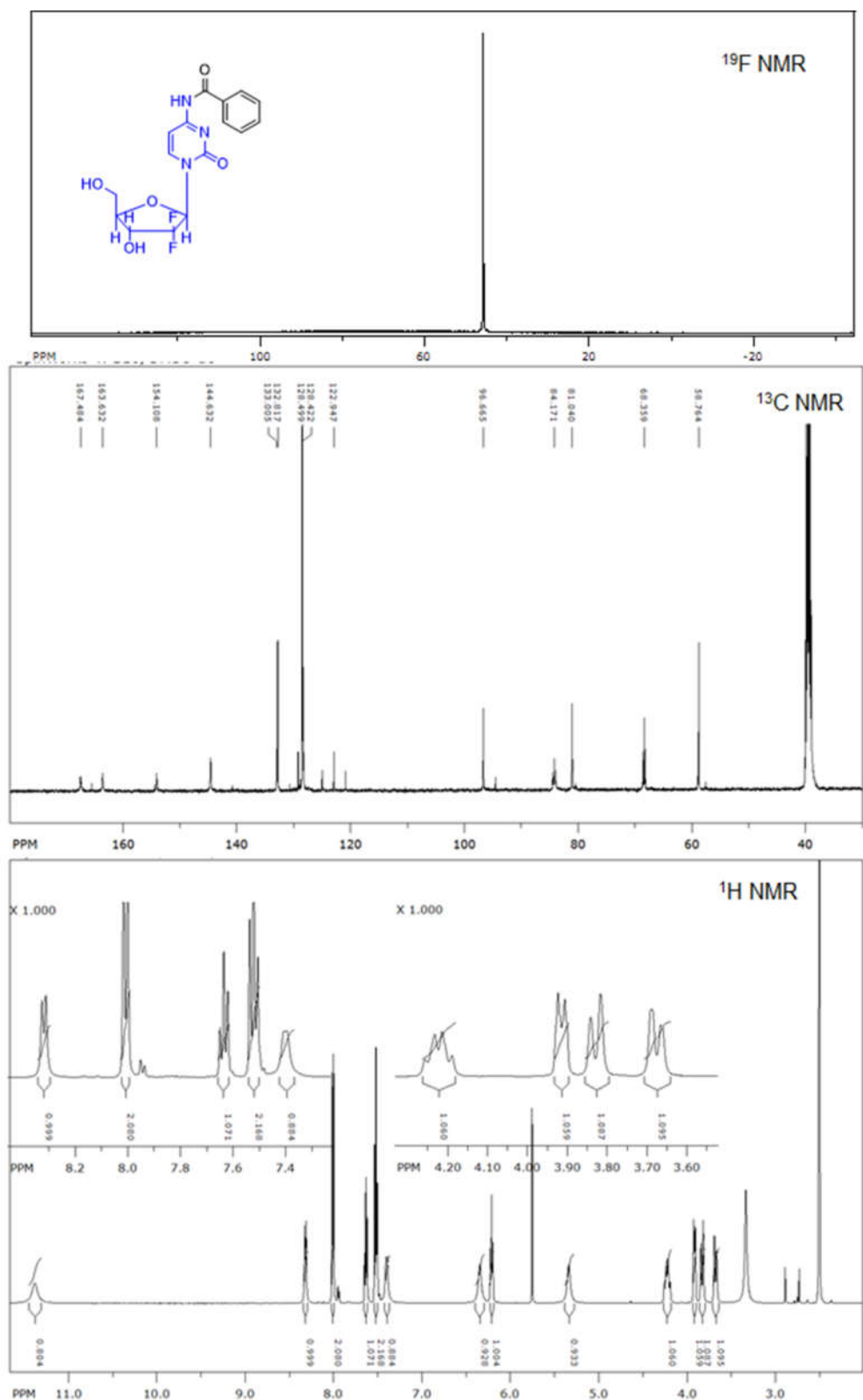


Figure S1. Characteristics of the 4-N-benzoyl-2'-deoxy-2',2'-difluorocytidine.

*4-N-(2-dimethylaminoethyl)-2'-deoxy-2',2'-difluorocytidine (3)*

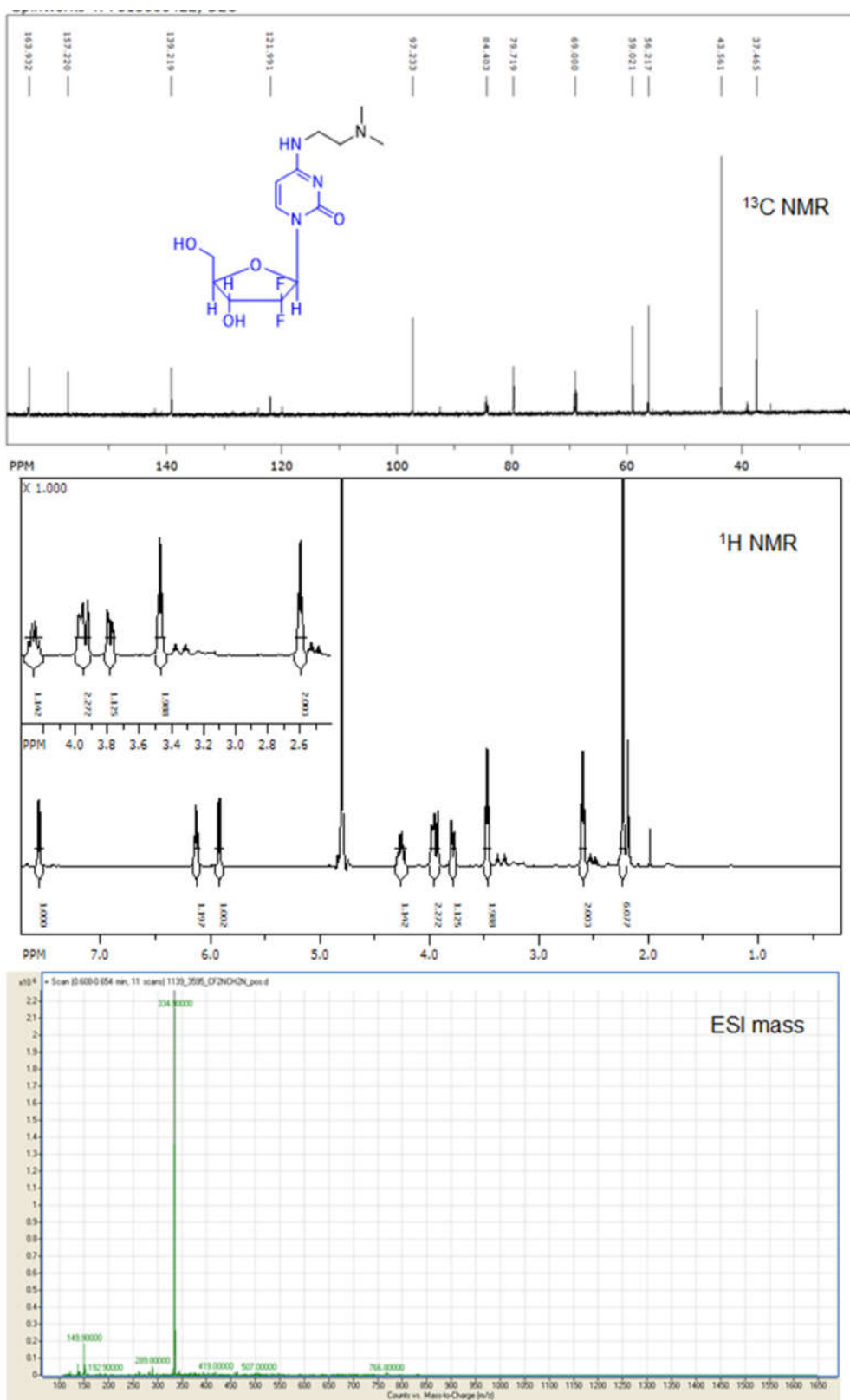


Figure S2. Characteristics of the 4-N-(2-dimethylaminoethyl)-2'-deoxy-2',2'-difluorocytidine

$H^+[Conjugate\ 5]$

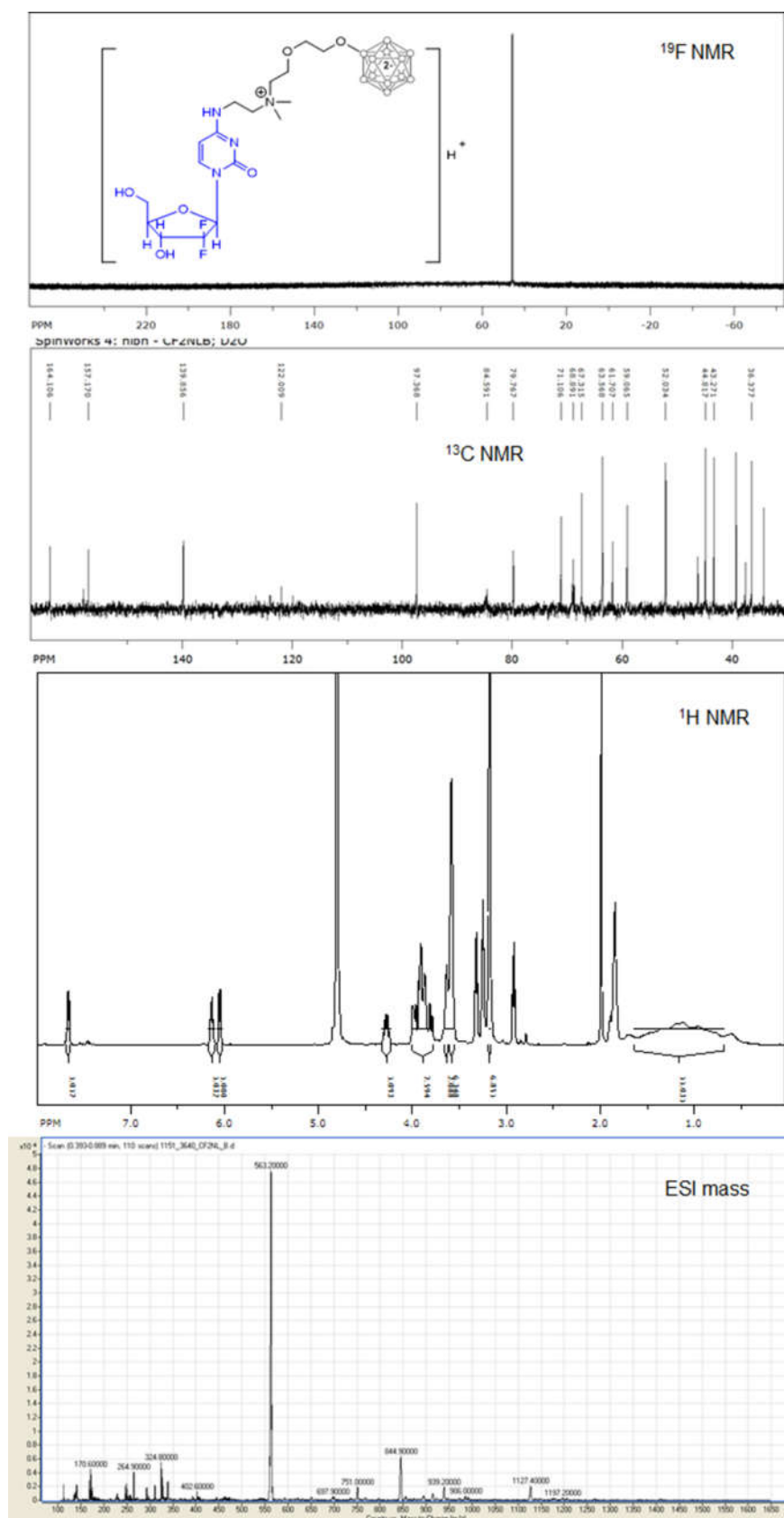


Figure S3. Characteristics of the  $H^+[Compound\ 5]$ .

[Compound 6](TEA)<sub>3</sub>

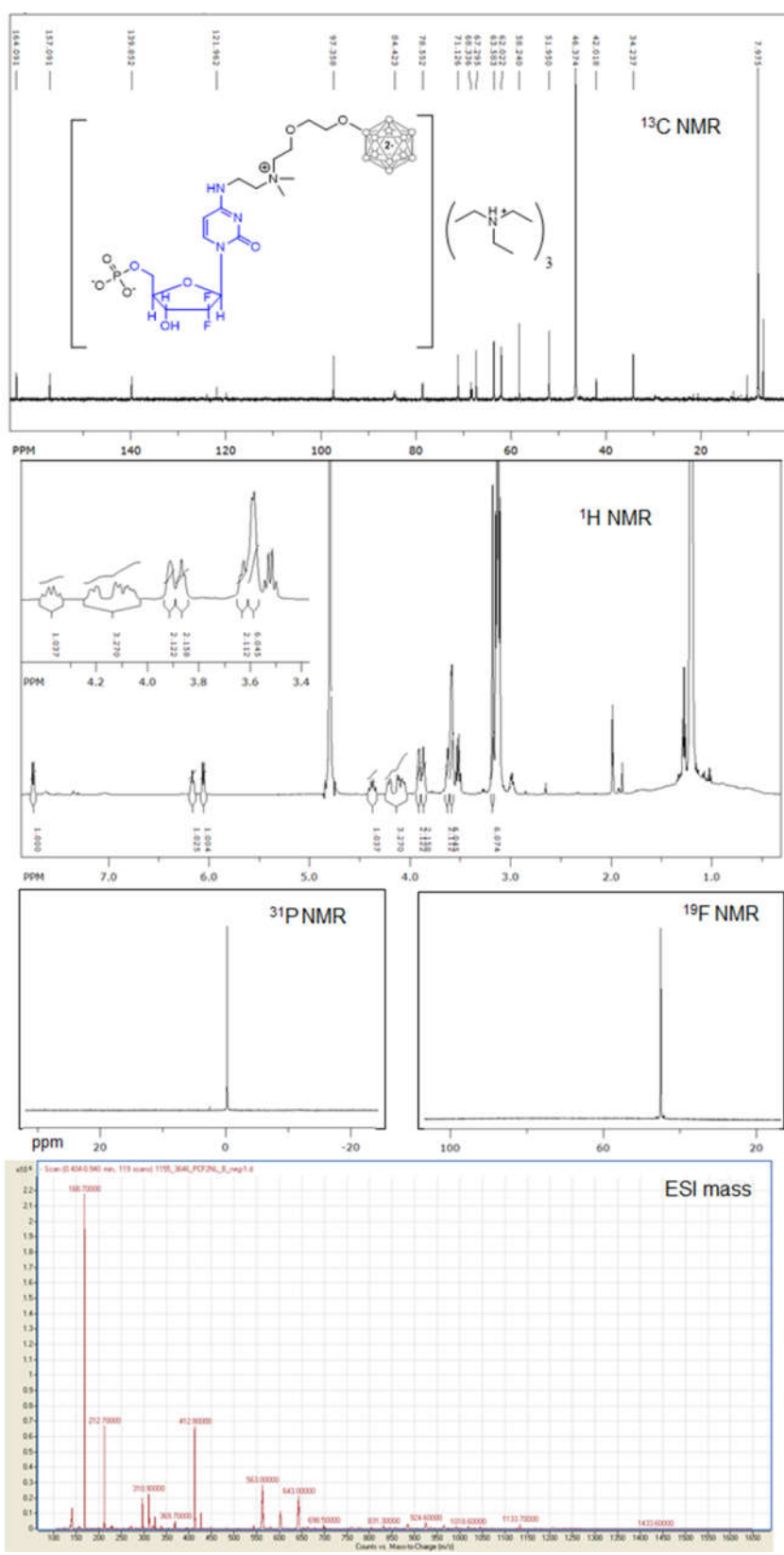


Figure S4. Characteristics of the [Compound 6](TEA)<sub>3</sub>.

[Compound 7](TEA)<sub>2</sub>

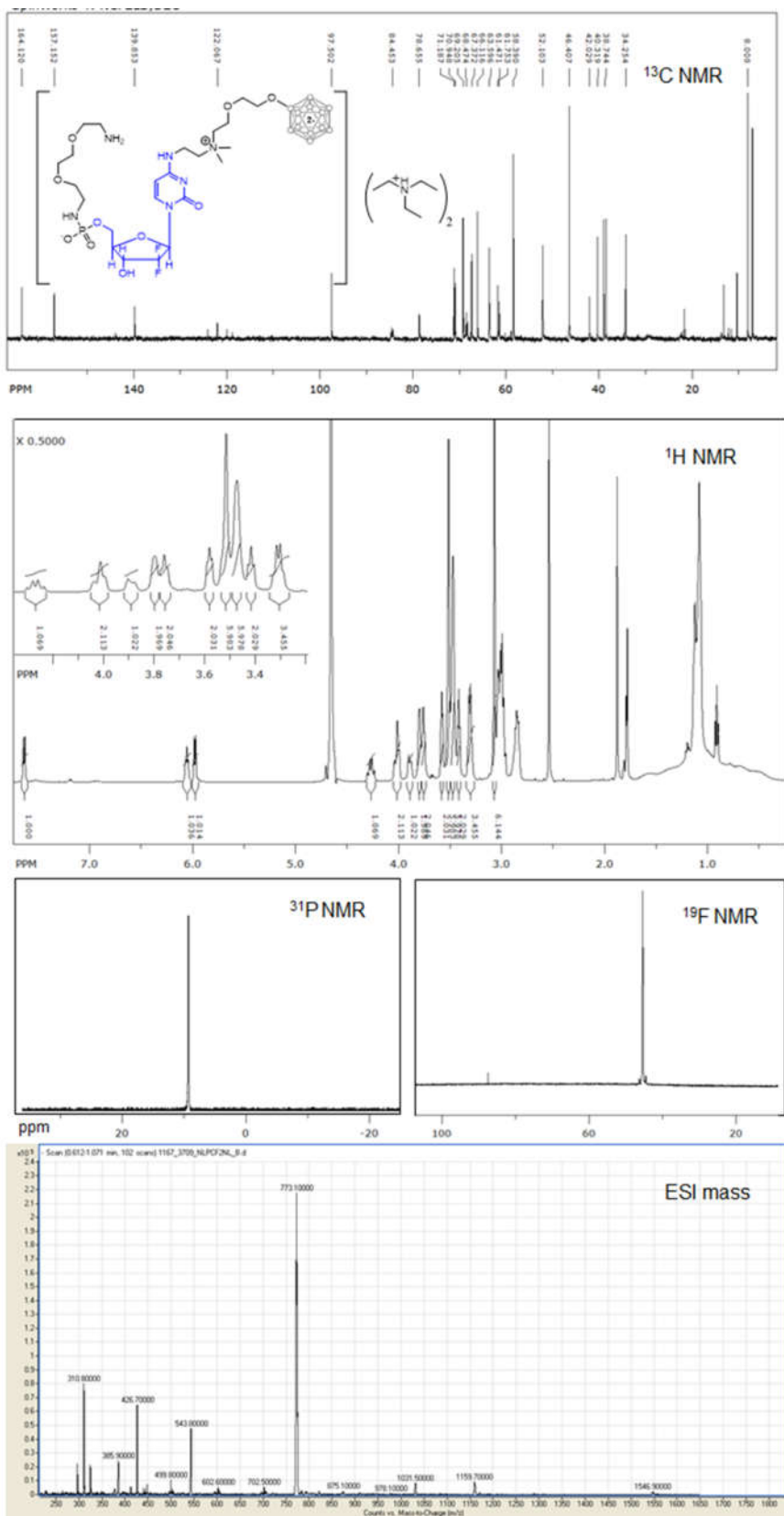


Figure S5. Characteristics of the [Compound 7](TEA)<sub>2</sub>.

[Compound 1](TEA)<sub>2</sub>

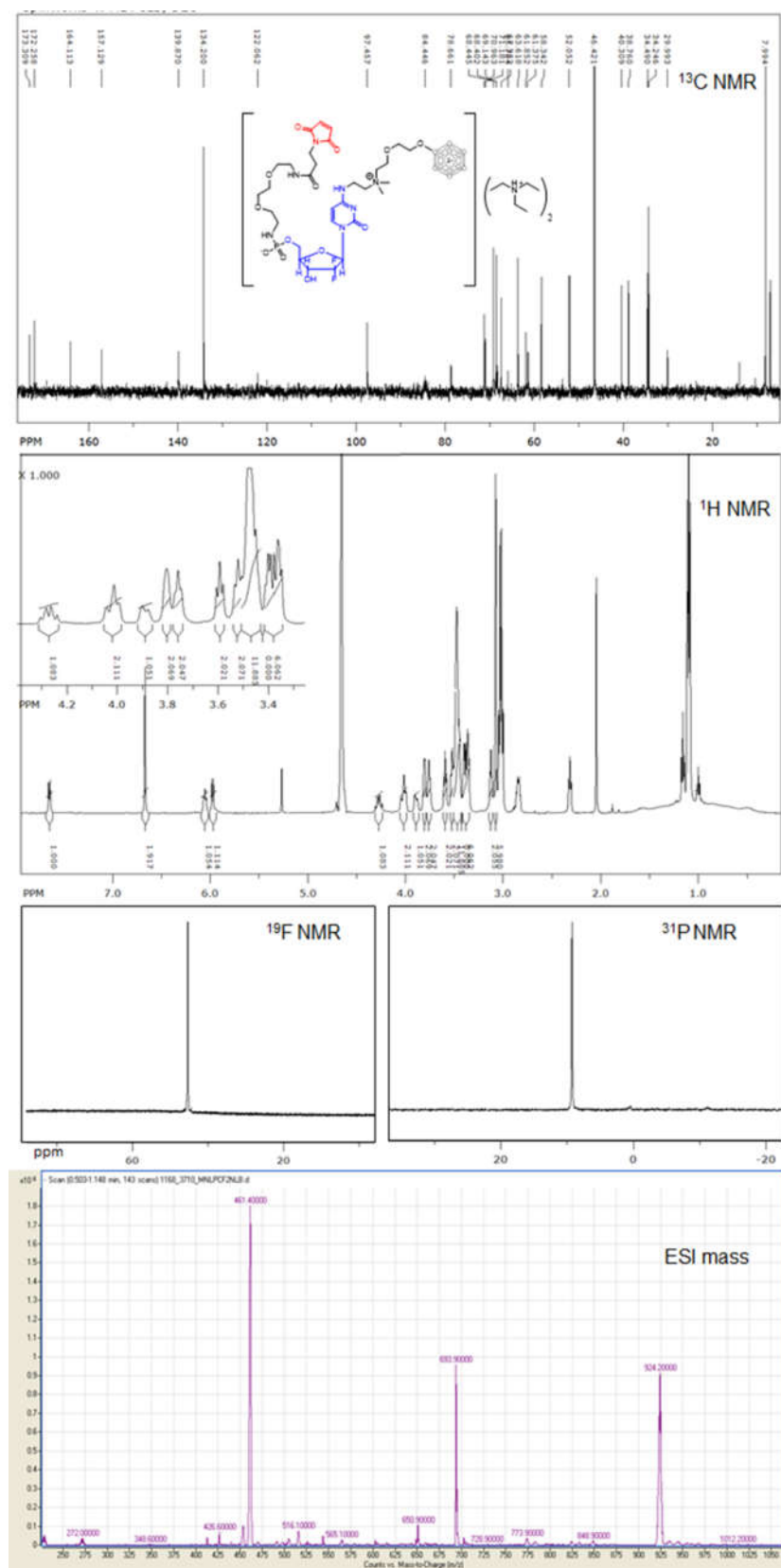


Figure S6. Characteristics of the [Compound 1](TEA)<sub>2</sub>.

*Compound 9*

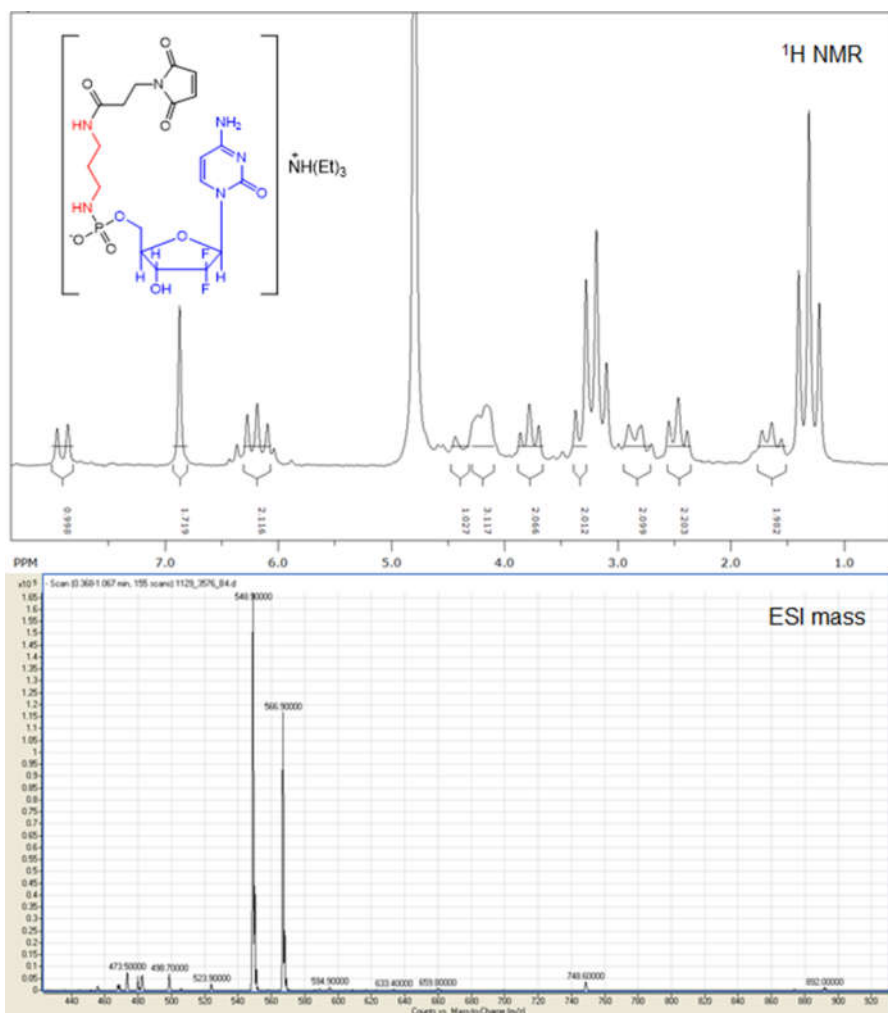


Figure S7. Characteristics of the [Compound 9](TEA).

<sup>1</sup>H NMR ( $D_2O$ ): 7.91 (1H, d,  $J$  7.6, H6), 6.88 (2H, s, CH=CH), 6.31-6.07 (2H, m, H1', H5), 4.47-4.31 (1H, m, H3'), 4.30-4.09 (3H, m, H4', H5'), 3.78 (2H, t,  $J$  6.5, CH<sub>2</sub>N), 3.39-3.28 (2H, m, CH<sub>2</sub>NHCO), 2.95-2.71 (2H, m, CH<sub>2</sub>CO), 2.46 (2H, t,  $J$  6.5, CH<sub>2</sub>NHP), 1.64 (2H, t,  $J$  6.8, CH<sub>2</sub>). [M-H]<sup>-</sup> calcd. for C<sub>19</sub>H<sub>24</sub>F<sub>2</sub>N<sub>6</sub>O<sub>9</sub>P<sup>-</sup> 549.13; found 548.90.

*Compound 9\**

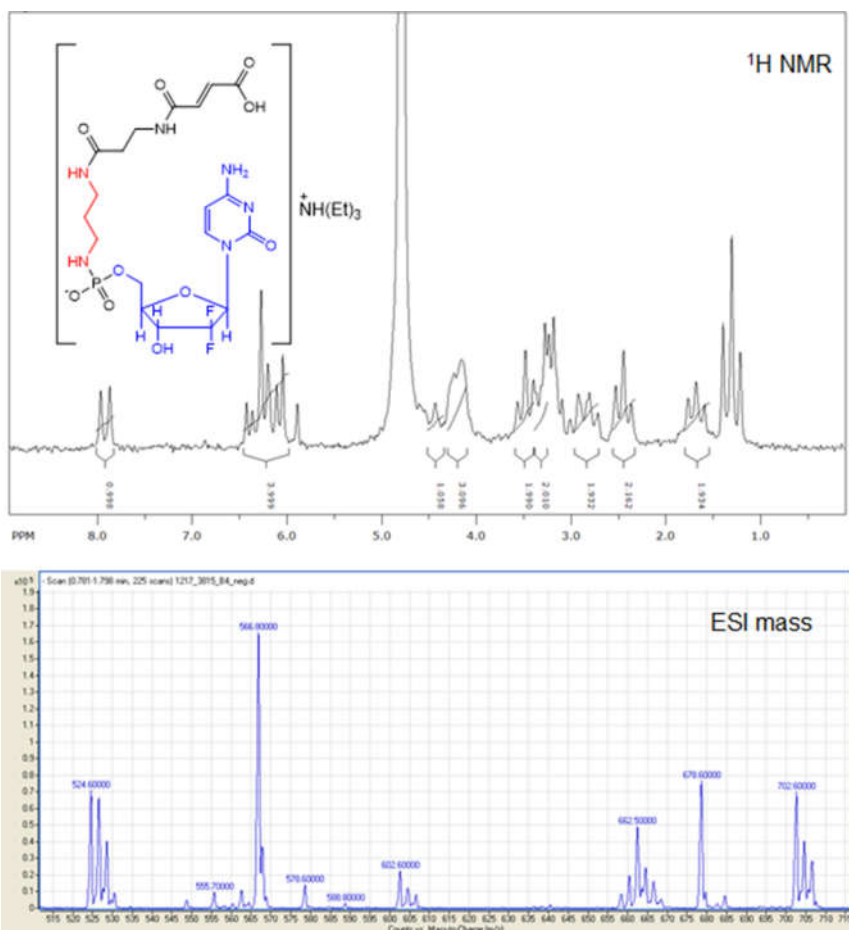


Figure S8. Characteristics of the [Compound 9\*](TEA).

$^1\text{H}$  NMR ( $\text{D}_2\text{O}$ ): 7.92 (1H, d,  $J$  7.6, H6), 6.46-5.98 (4H, m,  $\text{CH}=\text{CH}$ , H5, H1'), 4.52-4.34 (1H, m, H3'), 4.30-4.10 (3H, m, H4', H5'), 3.48 (2H, t,  $J$  6.7,  $\text{CH}_2\text{NH}$ ), 3.38-3.25 (2H, m,  $\text{CH}_2\text{NHCO}$ ), 2.96-2.71 (2H, m,  $\text{CH}_2\text{CO}$ ), 2.45 (2H, t,  $J$  6.7,  $\text{CH}_2\text{NHP}$ ), 1.68 (2H, t,  $J$  6.8,  $\text{CH}_2$ ).  $[\text{M}-\text{H}]^-$  calcd. for  $\text{C}_{19}\text{H}_{26}\text{F}_2\text{N}_6\text{O}_{10}\text{P}^-$  567.14; found 566.90.

*Compound 10*

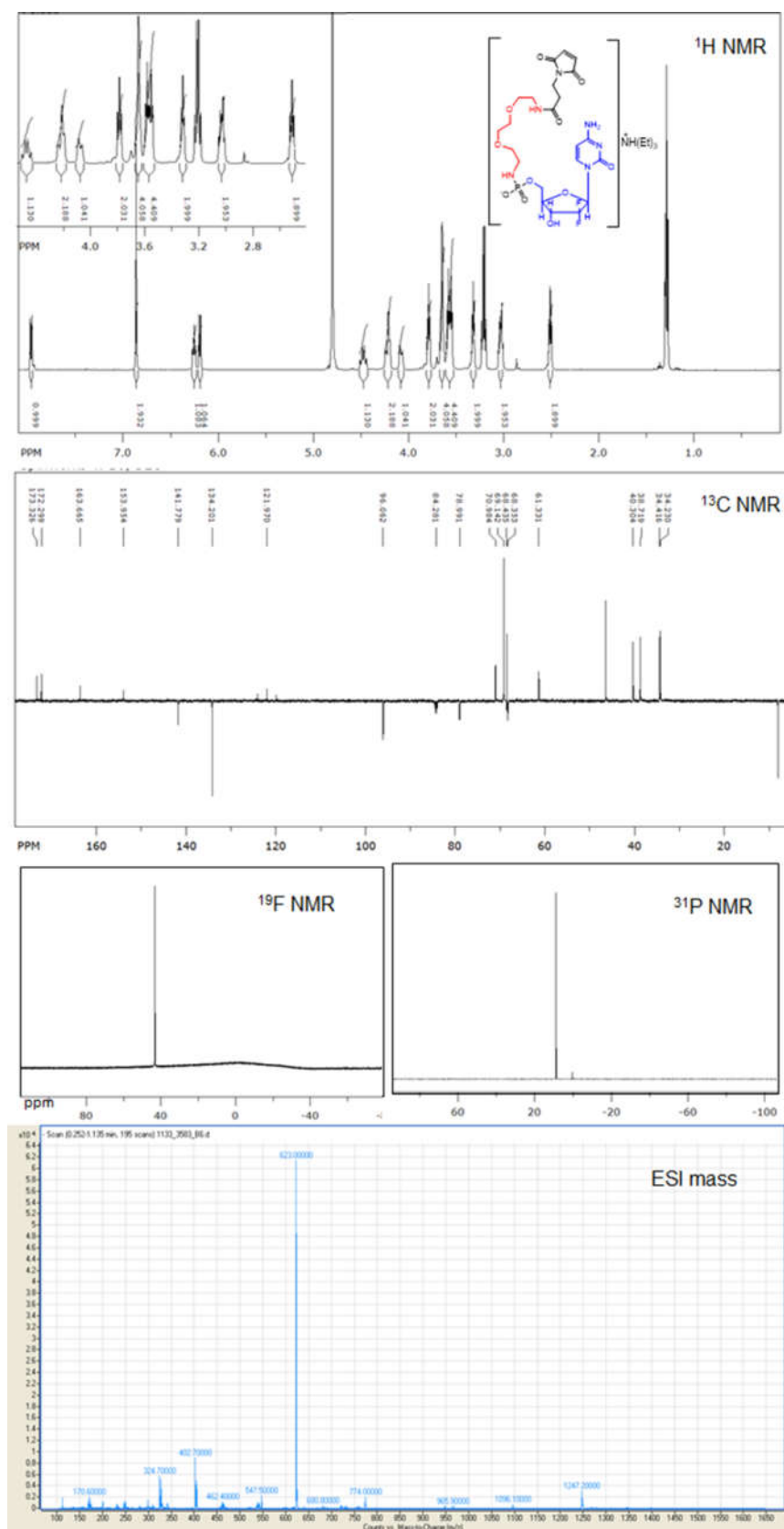


Figure S9. Characteristics of the [Compound 10](TEA).

<sup>1</sup>H NMR ( $\text{D}_2\text{O}$ ): 7.97 (1H, d,  $J$  7.7, H6), 6.86 (2H, s,  $\text{CH}=\text{CH}$ ), 6.26 (1H, t,  $J$  7.1, H1'), 6.20 (1H, d,  $J$  7.7, H5), 4.52-4.43 (1H, m, H3'), 4.26-4.18 (2H, m, H5'), 4.11-4.05 (1H, m, H4'), 3.79 (2H, t,  $J$  6.3,  $\text{CH}_2\text{N}$ ), 3.67-3.62 (4H, m,  $\text{CH}_2\text{O}$ ), 3.58 (2H, t,  $J$  5.5,  $\text{OCH}_2\text{CH}_2\text{O}$ ), 3.55 (2H, t,  $J$  5.5,  $\text{OCH}_2\text{CH}_2\text{O}$ ), 3.32 (2H, br t,  $J$  5.3,  $\text{CH}_2\text{NHCO}$ ), 3.05-3.01 (2H, m,  $\text{CH}_2\text{NHP}$ ), 2.51 (2H, t,  $J$  6.4,  $\text{CH}_2\text{CONH}$ ). <sup>13</sup>C NMR ( $\text{D}_2\text{O}$ ): 173.33, 172.30, 163.67, 153.95, 141.78, 134.20, 121.97 (t,  $J_{\text{CF}}$  259), 96.06, 84.28 (t,  $J_{\text{CF}}$  23), 78.99, 70.98, 69.14, 68.44, 68.35 (t,  $J_{\text{CF}}$  23), 61.33, 40.30, 38.72, 34.42, 34.23. <sup>19</sup>F NMR ( $\text{D}_2\text{O}$ ): 43.14 (br s,  $\text{CF}_2$ ). <sup>31</sup>P NMR: 8.67 (s). [M-H]<sup>-</sup> calcd. for  $\text{C}_{22}\text{H}_{30}\text{F}_2\text{N}_6\text{O}_{11}\text{P}^-$  623.17; found 623.00.

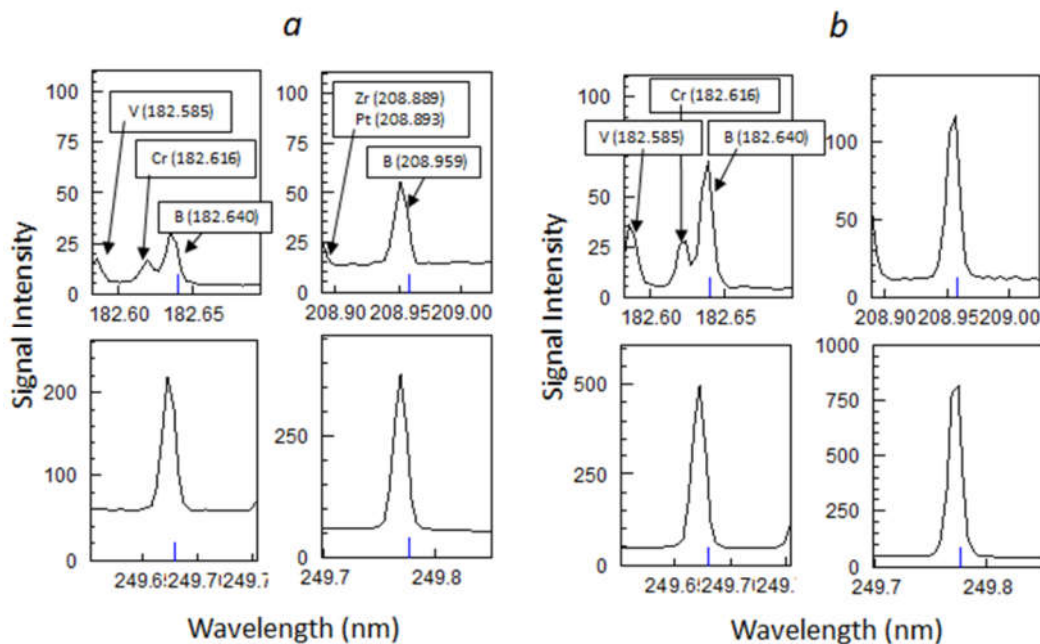


Figure S10. Inductively coupled plasma atomic emission spectrometry (ICP AES) for HSA-Cy5-HcyTFAc-GCB<sub>12</sub>H<sub>11</sub> (a) and HSA-Cy7-HcyTFAc-GCB<sub>12</sub>H<sub>11</sub> (b). Boron spectral lines 182.640, 208.959, 249.678 and 249.773 nm.

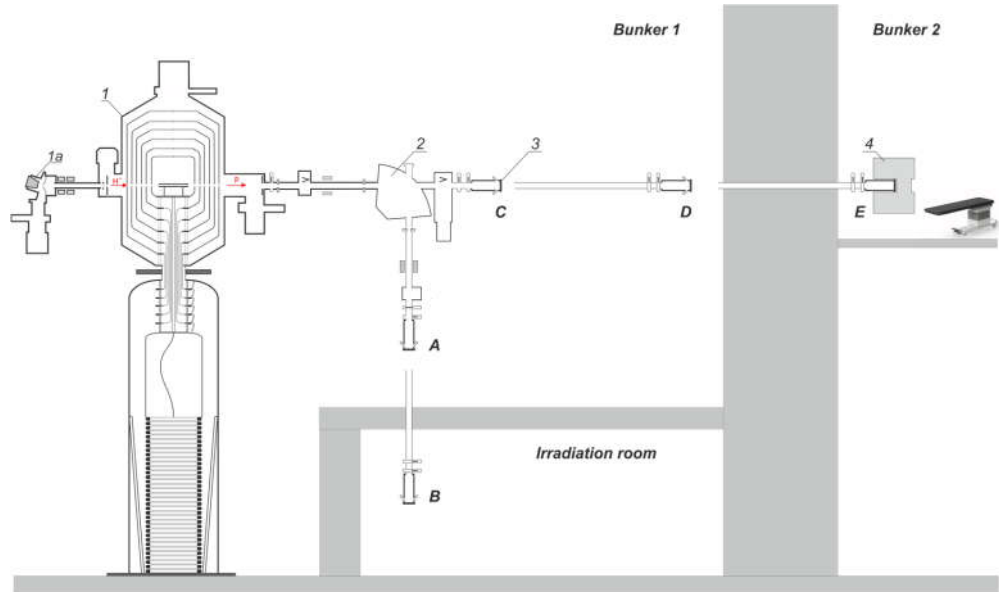


Figure S11. Layout of the experimental facility: 1 – vacuum insulated tandem accelerator, 2 – bending magnet, 3 – lithium target, 4 – beam shaping assembly. A, B, C, D, E – lithium target placement positions.